Cobalt Nanoparticles To Enhance Anaerobic Digestion of Cow Dung: Focusing On Kinetic Models For Biogas Yield And Effluent Utilization

Taha Abdelfattah Mohammed Abdelwahab (taha_abdelfattah40@yahoo.com)
College of Agricultural Engineering and Technology, OUAT https://orcid.org/0000-0002-4916-8117
Mahendra Kumar Mohanty
College of Agricultural Engineering and Technology
Pradeepta Kumar Sahoo
College of Agricultural Engineering and Technology
Debaraj Behera
College of Agricultural Engineering and Technology

Research Article

Keywords: Anaerobic digestion, Manure treatment, Cobalt nanoparticles, Methane production, Hydrogen sulfide, Effluent

Posted Date: August 3rd, 2021

DOI: https://doi.org/10.21203/rs.3.rs-660712/v1

Abstract

The impacts of Co nanoparticles (NPs) on the anaerobic digestion (AD) of cow dung were investigated using kinetic models (modified Gompertze, logistic, and first-order) and experimental measurements. The deviation between the predicted and measured data for biogas yield with modified Gompertze and logistic models were (0.66%-2.26%) and (1.43%-4.19%), respectively. The addition of Co NPs (1-3 mg/L) improved the hydrolysis rate (*K*) value by (66.66%-144%) compared with the control. Furthermore, effluent with Co NPs showed remarkable fertility (4.63%-5.32%). The combination of kinetic models and experimental measurements can effectively quantify the impact of Co NPs on AD performance and provide an informed choice for industrial production.

Highlights

- Introduction of Co NPs (1-2 mg/L) can improve biogas production by 6.82%-14.81%.
- Three kinetic models (modified Gompertze, logistic, and first-order) are employed to predict biogas yield and hydrolysis rate.
- Predicted data (0.66%-2.26%) of modified Gompertze model is closer to measured data than logistic model.
- First-order model fitting proves Co NPs improve the hydrolysis rate (K) value by (66.66%-144%).
- The selected kinetic models fit well with the experimental data (R^2 >0.98).

Introduction

Global economic progress in the twenty-first century has resulted in widespread use of fossil fuels. The widespread usage of fossil fuels has resulted in massive CO_2 emissions as a byproduct of combustion. Furthermore, the overall amount of solid and organic waste generated is increasing at an even faster rate, posing severe environmental consequences if not properly treated. Nowadays, renewable energy sources based on biomass have become increasingly important, with a trend to partially replace fossil fuel consumption by converting organic waste into clean energy, such as the use of anaerobic digestion (AD) to convert organic waste such as animal manure (Chowdhury et al., 2020), agricultural residues (Tamburini et al., 2020), food waste (Bedoi et al., 2020), and sewage sludge (Zhang and Zang, 2019).

Hydrolysis, acidogenesis, acetogenesis, and methanogenesis are the four key processes in AD (Madsen et al., 2011). With the help of fermentation bacteria, big polymers combine with water to generate smaller organic compounds such as glucose, fatty acids, and amino acids, which is the first stage in the AD process. Acidogenesis is the second step, in which smaller organic molecules are converted into VFAs, alcohols, lactic acid, CO_2, H_2, NH_3, and H_2S by acidogenic bacteria. The third phase is acetogenesis, which involves acetogenesis bacteria converting VFAs to acetate, H_2, and CO_2. Methanogenesis is the final phase in biogas production, in which acetate, H_2, and CO_2 are transformed to CH_4 and CO_2 through acetoclastic and hydrogenotrophic methanogenesis, respectively (Kothari et al., 2014; Kiran et al., 2015).

In this sense, providing these bacteria with appropriate nutrients and a steady operational environment will help them digest organic waste efficiently (Facchin et al., 2013). Trace elements as micronutrients have been added to AD systems to provide more suitable circumstances for the microorganisms present in the digester (Abdelwahab et al., 2020a). Co has been found to be a significant trace mineral addition for the development of methanogenic bacteria throughout the AD process (Ajay et al., 2020). Co is required for methanogenic bacteria to degrade methanol (as a protein cofactor of vitamin) (Roussel et al., 2013). In addition, the usage of Co is thought to be a significant element in the oxidation of acetate to CO_2 and H_2, resulting in the hydrogenotrophic methanogenic process (Thauer et al., 2008; Romero-Guiza et al., 2016). Abdelsalam et al. (2016) used a batch AD system to examine the effect of Co NPs (20 nm) on biogas and CH_4 production from cattle manure slurry. Treatment of the substrate with 0.5 and 1 mg/L Co NPs increased cumulative biogas production (36.5 % and 64.12 %, respectively) and CH_4 production as compared to the control (biogas, 33.0 L; methane, 16.8 L) (41.6 % and 41.8 %, respectively). These findings are consistent with those of Zaidi et al. (2018), who reported that using 1 mg/L Co NPs during the AD of green microalgae boosted biogas generation by 9% over a control experiment. Furthermore, the aforementioned additives shorten the time it takes to reach peak biogas and CH_4 production. However, compared to the control condition, the addition of 2 mg/L Co NPs reduced both biogas and CH_4 production by 5.2 % and 14.54 %, respectively. Poultry litter treated with 1.4, 2.7, and 5.4 mg/L Co NPs increased CH_4 generation by 29.0 %, 26.05 %, and 30 %, respectively (Hassanein et al., 2019). Another study used cattle manure as a substrate to investigate the use of 1 mg/L Co NPs in AD. Biogas and CH_4 production have increased by 71.2 % and 45.9%, respectively, as compared to control (Abdelsalam et al., 2016).

The downstream application of a lab-scale AD process necessitates kinetic analysis (Wang et al., 2016). The ideal process variables, such as the lag phase and hydrolysis constant, can be identified through kinetic model fitting. It also investigates the AD process's biogas yield rate and potential (Donoso-Bravo et al., 2010; Mishra and Mohanty, 2018). The effects of Co NPs on AD were examined using both kinetic models and experimental observations, taking into account the above-mentioned advantages of kinetic model fitting.

Co NPs have been used in AD system and resulted in improved biogas production (Abdelsalam et al., 2017a and b). However, the impact of Co NPs on the kinetic for biogas production and effluent utilization is not investigated, which is the key distinction from the present work. The following were the specific objectives of the study: (1) to determine the optimal concentrations of Co NPs on biogas and CH_4 production, H_2S mitigation, Ph, volatile fatty acids (VFAs), and total alkalinity (TA) variation, total solids (TS), and volatile solids (VS) removal rates during AD of cow dung; (2) to predict the kinetic parameters (maximum biogas production rate and potential, lag phase, and hydrolysis constant) of biogas yield using the modified Gompertze model, logistic model, and first-order kinetic model; (3) to investigate the feasibility of effluent utilization by fertilizer analysis.

Materials And Methods

2.1. Nanoparticles dispersion preparation

Co nanopowder was acquired from Nano research lab, Jharkhand, India. Stock solution of Co NPs was prepared by dispersing nanopowder into MiliQ water (Conductivity of 18.2 MΩ/cm at 25°C). The stock was then ultra-sonicated at 20 KHz at 38°C for 1h to break aggregates and disperse Co NPs into the solution. To prevent photocatalytic and thermal reactions, the Co NPs dispersion was kept in dark condition at 4°C and used within 24 h of preparation (Nguyen et al., 2015).

2.2. Inoculum and substrate preparation

The inoculum, anaerobic cow dung, had been cultured for 30 days in a lab-scale batch bio-digester under mesophilic conditions (33 ± 0.5°C). The substrate in this study was fresh cow dung obtained from the cattle farm of Odisha University of Agriculture and Technology in Bhubaneshwar, Odisha, India. On a weight basis, the substrate was made by mixing distilled water with fresh cow dung in a 1:1 ratio. For each reactor, a 1:1 by volume ratio of substrate to inoculum was used (slurry). Table 1 lists the key properties of the substrate, inoculum, and slurry employed in this study.

Table 1 The characteristics of substrate, inoculum, and slurry.

Parameter	Substrate (cow dung + water)	Inoculum	Slurry (Substrate + inoculum)
TS (%)	9.41± 0.32	9.05 ± 0.42	9.30 ± 0.21
VS (%)	82.60 ± 1.7	85.24 ± 1	83.30 ± 2
VFAs (mg/L)	4050 ± 32	3300 ± 44	3750 ± 50
TA (mg/L $CaCo_3$)	4200 ± 73	4500 ± 100	4300 ± 50
VFA/TA ratio	0.96 ± 0.01	0.73 ± 0.01	0.89 ± 0.01
pH	6.45 ± 0.02	7.14 ± 0.07	6.60 ± 0.05

2.3. AD experiment design

At 33 ± 0.5°C, the AD experiments were carried out in several identical 2000-mL digesters with a working capacity of 1000 mL. Depending on the test setting, each digester included inoculum (44.86 g dry matter), substrate (44.55 g dry matter), and varying amounts of Co NP additions. Three Co NPs concentrations were used 1 mg/L (0.06 mg/g VS), 2 mg/L (0.12 mg/g VS), and 3 mg/L (0.18 mg/g VS). In the control digester, only inoculum and substrate were used, with no Co NPs additions. Each test condition was carried out three times. Each digester's gas vent was connected to a biogas collecting device, and the volume of biogas produced was measured using the displacement method. Please see the previous articles for a more complete discussion of the experimental devices (Abdelwahab et al., 2020b, 2021 a, b). The AD tests were run in batch mode for 30 days before being stopped when daily biogas production

fell below 1% of total biogas production. Three times a day, each reactor was manually shaken. Each digester's gas and liquid samples were gathered for analysis on a regular basis. A flow diagram was used to depict the experimental processes (Fig. 1).

2.4. Analytical methods and data calculation

The volume of biogas was determined using the liquid displacement method, and the contents of CH_4 and H_2S were determined using a portable biogas analyzer (SR 2012, India). Total solids (TS), volatile solids (VS), and pH were measured every 10 days. The TS % and VS % were calculated using standard procedures (section 2540G) (ABHA, 2005); pH was tested using Thermo Fisher Scientific (XL 600, Japan). An inductively coupled plasma optical emission spectrometer was used to measure total Co, K, and P before and after the experiments (ICP-OES, Perkin Elmer, Avio 200, USA). Co was prepared using nitric acid digestion standard procedures section 3030F, APHA (1995), whereas K and P were prepared using nitric acid-hydrochloric acid digestion standard procedures section 3030H, APHA (1995). Using a micro elemental analyzer and simultaneous CHNS determination, total C, N, S, and H were determined before and after experiments (UNICUBE, Germany). After the experiments, Fourier transform infrared spectroscopy was used to characterise the organic content in the effluent samples (dry samples) (FTIR, PerkinElmer spectrum, version 10.4.3., USA). A Carl-Zeiss Merlin II field emission scanning electron microscope was used to characterise the surface morphology and particle size of Co NPs (FESEM).

The cumulative biogas yield of each bio-digester was mathematically calculated, and the results were expressed as cumulative biogas yield per g VS added (Zhang et al., 2014).

The VS removal efficiency was calculated by using Eq. (1) (Ali et al., 2019):

$$VS_{removal\ efficiency}(\%) = 100 \times \frac{VS_0 - VS_d}{VS_d} \quad (1)$$

Where VS_0 is volatile solids in substrate added (slurry) and VS_d volatile solids in the effluent (after AD).

2.5. Kinetics analytical methods

2.5.1 Kinetics of biogas production

The calculation and comparison of biogas production kinetic during digestion of slurry with different Co NPs concentrations were modeled via modified Gompertz model Eq. (2) (Syaichurrozi and Sumardiono, 2013) and logistic function model Eq. (3) (Deepanraj et al., 2017). This allowed the estimation of the lag phase time (λ, d), the maximum biogas potential production (M_{max}, mL/g VS), and the maximum biogas production rate (R_{max}, mL/g VS/d).

$$M(t) = M_{max} \times exp\left[-exp\left\{\frac{R_{max} \times e}{M_{max}}(\lambda - t) + 1\right\}\right] \quad (2)$$

$$M(t) = \frac{M_{max}}{1 + exp\left[4R_{max}\frac{(\lambda - t)}{M_{max} + 2}\right]} \quad (3)$$

Where *M(t)* cumulative biogas production (mL/g VS) at time t (30 days); M_{max} is the maximum biogas potential production (mL/g VS); R_{max} is the maximum biogas production rate (mL/g VS/d); λ is the lag phase (d); *t* is total digestion time (d).

2.5.2 Kinetics of slurry hydrolysis

The calculation and comparison of the hydrolysis rate constant (*k*) of slurry with different Co NPs concentrations were modeled via first-order kinetic model Eq. (4).

$$L_t = l_{max} . (1 - e^{-kt}) \quad (4)$$

Where *Lt* is cumulative biogas production (mL/g VS) at time t (30 days); L_{max} is the maximum biogas potential production (mL/g VS); *k* is the hydrolysis rate constant (d^{-1}); *t* is time (d).

A second order Akaike Information Criterion (AIC) test was used to determine which model best matches the experimental data (Rawlings et al., 2001). An AIC value can be positive or negative, and the sign has no significance because it can be expressed in multiple units. The difference between the AIC values was used to compare models, with the model with the smallest AIC values being considered the most likely to be true. Eqs. (5) were used to compute the AIC value (Wong and Li, 1998).

$$\mathrm{AIC} = \begin{cases} Nln\frac{RSS+2n}{N}, when\ \frac{N}{n} \geq 40 \\ Nln\frac{RSS}{N} + 2n + \frac{2n(n+1)}{N-n-1},\ when\ \frac{N}{n} < 40 \end{cases} \quad (5)$$

Where *N* number of points; *RSS* residual sum of square; *n* number of model parameters.

2.6. Statistical analysis

Statistical analysis was performed using the SPSS Statistic Software version 20 (IBM Co.) with p-values calculated at a 95% confidence level.

Results And Discussion

3.1 Surface morphology and particle size characterization of Co nanoparticles

The surface morphology and structure of Co NPs were investigated using FESEM. As shown in Fig. 2, Co NPs are irregular block particles with individual sizes ranging from 70 to 104 nm.

3.2 Impacts of Co nanoparticles on biogas yield

When the substrate was exposed to 1, 2, and 3 mg/L of Co NPs, the starting of biogas yield was improved, as shown in Fig. 3. The addition of 1, 2, and 3 mg/L Co NPs, in particular, increased biogas yield startup by 23.0 %, 53.1 %, and 23.0.3 %, respectively, in the first 5 days of digestion. The addition of Co NPs speeds up the process of reaching peak biogas production. On day 6, the 2 mg/L Co NPs

produced the highest daily biogas yield, with approximately 42.6 mL/g VS. However, the greatest daily biogas production of the control was 34.0 mL/g VS on day 19.

As shown in Fig. 4, the addition of 2 mg/L Co NPs increased biogas yield to 6767.5 mL/g VS, which is greater than the biogas yielded by the control, 1 mg/L Co NPs, and 3 mg/L Co NPs, which were 589.2, 629.5, and 602.3 mL/g VS, respectively. According to the statistical analysis, the addition of 1 and 2 mg/L Co NPs increased cumulative biogas yield by 6.83 % and 14.81 %, respectively, as compared to the control. However, there were no significant differences in cumulative biogas production with 3 mg/L Co NPs compared to the control (p-value = 0.430). The addition of Co NPs speeds up the process of reaching peak biogas production (Fig. 4). After 30 days of fermentation, the control treatment yielded 589.2 mL/g VS, but the Co NPs treatment (2 mg/L) yielded 595.8 mL/g VS after 22 days, indicating that 22 days may be sufficient (HRT).

3.3 Impacts of Co nanoparticles on methane yield

According to the cumulative CH_4 production curves, adding 1 mg/L Co NPs to the substrate increased CH_4 yield to 33.3 mL/g VS, which is significantly higher ($p < 0.05$) than the CH_4 produced by control, 2 mg/L Co NPs, and 3 mg/L Co NPs, which produced 18.59, 29.07, and 28.75 mL/g VS of CH_4, respectively. The addition of 1, 2, and 3 mg/L of Co NPs enhanced the CH_4 yield by 79.12 %, 56.37 %, and 54.65 %, respectively, when compared to control ($p < 0.05$). Furthermore, as shown in Fig. 4, no significant variations in CH_4 yield were attained when 2 mg/L Co NPs and 3 mg/L Co NPs were added to the substrate (p-value = 0.857).

The results of the experiment correspond with those of Zandvoort et al. (2006), who found that 0.8 mg/L Co is the best dosage. Furthermore, when the substrate was exposed to 1 mg/L Co NPs, the greatest CH_4 yield was achieved, which accords with Abdelsalam et al. (2016), who observed that the presence of 1 mg/L Co NPs boosted CH_4 production by 86 % when compared to the control condition (manure without NP additives). Furthermore, the increase in CH_4 in our results using 1 mg/L Co was similar with the findings of Qiang et al. (2012), Demirel and Scherer (2011), and Feng et al. (2010), who all concluded that Co is an essential metal for methanogenesis because it acts as a metallic enzyme activator.

3.4 Effects of Co nanoparticles on hydrogen sulfide yield

As seen in Fig. 5, Co NPs significantly reduce cumulative H_2S production ($p < 0.05$) for all concentrations evaluated when compared to control. When compared to control, cumulative H_2S generation of 1, 2, and 3 mg/L Co NPs was reduced by 15.38 %, 13.20 %, and 57.89 %, respectively. Furthermore, the maximum H_2S removal efficiency of 57.89 % was achieved with 3 mg/L Co NPs added. The removal efficiency of Co NPs at 1 and 2 mg/L was 15.38 % and 13.20 %, respectively.

The results are better than those of Hassanein et al. (2019), who reported that using 5.4 mg/L Co NPs improved H_2S removal effectiveness by 6.79 %. It's possible that the variation in findings is due to the different substrate types. Co NPs effectively reduced H_2S emissions in all treated bio-digesters, according

to these findings. The precipitation of metal sulphide (Boer et al., 2014; Trifunovi et al., 2016) is one possible reason for the reduction of H_2S emissions in our investigation. With 1 mg/L of Co NPs and 2 mg/L of Co NPs, there were no significant changes in H_2S removal effectiveness (p-value = 0.548).

3.5 Effects of Co nanoparticles on pH, volatile fatty acids and total alkalinity

To begin, the dynamic shift in pH during AD represented the effect of Co NPs on the stability of the AD process. As seen in Fig. 6, there are two stages to the pH variations. pH increased in the first stage (from the beginning of the experiment to day 20). Furthermore, the maximum pH value was 7.3 both on Day 20 and with 1 mg/L of Co NPs.

The increase in pH could be related to i) the widespread usage of VFAs in AD systems; ii) the reaction between Co and organic molecules in the medium, which could result in an increase in pH. As a result of the aforementioned reaction, the substrate under AD will be depleted of hydrogen ions (H+), causing the pH of the substrate to rise. Furthermore, collecting CO_2 prevents the production of (H_2CO_3) inside the substrate, which raises pH (Amen et al., 2018). The pH drops throughout the second stage (from days 20 to shut down) due to the accumulation of VFAs (Chen et al., 2008).

Figure 7 shows the variation in volatile fatty acids (VFAs) concentrations of 1, 2, and 3 mg/L Co NPs. VFAs have two stages throughout the experimental period. The VFAs concentration showed a significant drop trend at the early stage (during the first 20 days of digestion time) for all Co NPs additions, with the highest VFAs degradation of 2800 mg/L with 2 mg/L Co NPs. This indicated that I once microorganisms adapted to the Co NPs environment, Co NPs offered an effective electron donor to boost microbial metabolism; and ii) the addition of track elements such Co may reduce the initial VFAs accumulation during the AD (Bayr et al., 2012; Wei et al., 2014).

The VFAs concentration increased with all Co NPs concentrations in the final stage (during the last 10 days of digestion), with the highest value of 4000 mg/L for 3 mg/L Co NPs. The increase in VFAs in the last stage could be related to total alkalinity decrees. The decrease in daily biogas production (Fig. 3) and pH value (Fig. 6) during the final stage could be attributed to the growth and accumulation of VFAs. Previous research has shown that increasing and accumulating VFAs causes a drop in pH and biogas production (Liu et al., 2014; Romsaiyud et al., 2009). This implies that the pH, VFAs, and biogas production are all in agreement.

Figure 8 shows the total alkalinity (TA) profile, which is identical to that of pH. Before 20 days (from the commencement of the experiment to day 20), the TA showed an upward trend. This meant that the rise in substrate TA was due to Co NPs having a beneficial influence on VFA consumption. The TA revealed a pattern of declines after 20 days (from day 20 until shut down), which could be due to VFA creation (Ahn et al., 2010).

The average TA concentrations were 4950, 4900, 4725, and 4475 mg $CaCo_3$/L, respectively, when the substrate was treated to 1, 2, 3 mg/L Co NPs and control. With the addition of 1 mg/L Co NPs, the TA concentration was increased. Suanon et al. (2017) found that the TA concentration indicated the consumption of VFAs by methanogen bacteria, which resulted in increased CH_4 production. These findings show that TA concentration and cumulative CH_4 production in experiment results are in accord, especially when 1 mg/L Co NPs are introduced.

3.6 Effects of Co nanoparticles on total and volatile solids

When assessing the stability of the AD process, the degradation of TS and VS must be taken into account. To begin with, Fig. 9 shows the total solids (TS) content with 1, 2, and 3 mg/L Co NPs added in contrast to the control. During the digesting period, the TS content in all biodigesters and the control biodigester decreased. Control, 1, 2, and 3 mg/L Ni NPs have TS removal efficiencies of 12.04 %, 14.81 %, 16.25 %, and 14.81 %, respectively.

In comparison to control, Fig. 10 shows the VS content at varied concentrations of 1, 2, and 3 mg/L Co NPs. The volatile solids (VS) content curve followed a similar pattern throughout the experiment. Control, 1, 2, and 3 mg/L Co NPs have VS removal efficiencies of 11.55 percent, 12.16 percent, 11.85 percent, and 10.66 percent, respectively. Co nanoparticles increased the degradation of organic matter by boosting the capacity of methanogens bacteria to breakdown organics, as evidenced by the change in TS and VS content after the addition of Co NPs.

3.7 Effects of Co nanoparticles on the characterization of organic material and chemical composition of the effluent

The FTIR method is used to detect the characteristic vibrations of chemical bonds and chemical functions. Figure 11 shows the profile of the effluent FTIR spectrum after the substrates were exposed to 1, 2, and 3 mg/L Co NPs compared to the control. According to the literature, the main absorption peaks were: i) O-H stretching of the carboxylic and alcoholic groups at about 3450 cm^{-1}; ii) C-H stretching of the aliphatic at about 2900 cm^{-1}; iii) -COO- stretching of the carboxylic acid at about 1600 cm^{-1}; iv) C-O stretching of the carbohydrate at about 1100 cm^{-1}; v) C-O stretching of the carbohydrate at (Abdulla et al., 2010; Gamage et al., 2014). When varying concentrations of Co NPs were added, the intensity and shift of peaks changed when compared to the control peak. In particular, the prominent peak in the spectrum about 1100 – 950 cm^{-1} corresponds to the carbohydrate's C-O stretching.

The decreased carbohydrate is reflected in the intensity of this band in the spectra of the treated sample. In comparison to other treatments (2 and 3 mg/L Co NPs) and control, the presence of 1 mg/L Co NPs exhibited the lowest intensity of the C-O band. These findings indicated that i) the presence of 1 mg/L Co NPs may be enhancing the methanogenesis communities' ability to decompose the carbohydrate with

the formation of VFAs, resulting in increased CH_4 production; and ii) the highest cumulative CH_4 production and the FTIR spectrum of effluent with 1 mg/L Co NPs added are in agreement.

The effect of different concentrations of Co NPs on the chemical composition of the digestate was observed in Table 2. The presence of Co NPs increased sulfide content. Sulfide content increased by 3%, 3.6%, and 12.12% with 1, 2, and 3 mg/L Co NPs added compared to control, respectively. The presence of 3 mg/L Ni NPs decreases the H_2S production by 57.89% as shown in Fig. 5 compared with control.

Table 2 Chemical composition of the effluent with different concentrations of Co NPs.

Element	Before digestion	After digestion			
	Slurry	Control	1 mg/L Co NPs	2 mg/L Co NPs	4 mg/L Co NPs
C %	39.63	40.91	40.27	40.27	41.03
H %	5.93	40.91	40.12	40.12	39.80
S %	0.31	0.33	0.340	0.342	0.373
Fe %	0.18	0.20	0.18	0.24	0.19
Ni %	$7.4*10^{-4}$	$8.2*10^{-4}$	0.041	$7.4*10^{-4}$	$1.1*10^{-3}$
Co %	$8.8*10^{-4}$	$2.0*10^{-4}$	$8.8*10^{-4}$	$2.7*10^{-3}$	$2.3*10^{-3}$

The bioavailability of organic matter and sulphate in AD stimulates the growth of SRB, which reduce sulphur to sulphide as a terminal electron receiver from a wide range of elements, including H_2, ethanol, formate, succinate, pyruvate, and lactate, resulting in reduced H_2S emission and increased sulphide content in the effluent in this study (Muyzer and Stams, 2008). In this case, Co NPs successfully reduced H_2S emissions by killing SRB, directly absorbing sulphur during digestion, or changing the polluting materials via a biochemical mechanism (Sevcu et al., 2011).

3.8 Fertility evaluation of effluent containing Co NPs

As shown in Fig. 12, the total nutrient (NPK) content of the digestate with 1, 2, and 3 mg/L Co NPs is 5.32 %, 4.68 %, and 4.63 %, respectively. Since all Co NPs concentrations had a total nutrient content of close to 5%, they can be utilized in conjunction with an artificial compound fertilizer. The digestates were dewatered and dried to provide a high-quality organic compound fertilizer. The physical and chemical features of soil can be improved with NPK organic compound fertilizer, which promotes the creation of soil aggregate structure and increases the activation of soil nutrients. It is obvious that when NPK organic compound fertilizer is employed, the crops demand significantly less water, and the area's chronic water shortage problem may be remedied. As a result, the AD digestate combined with the three Co NPs can be utilized to make an NPK organic compound fertilizer that improves plant height, root length, root diameter, and dry weight (Möller and Müller, 2012).

3.9 Kinetic analysis of biogas yield

Tables 3 and 4 show the findings obtained from the modified Gompertz and Logistic Function models, respectively. Figures 13 and 14 show a comparison of experimental and expected biogas yield using 1, 2, and 3 mg/L Co NP additions, as well as a control. The addition of 1,2, and 3 mg/L Co NPs boosted maximum biogas production rate (R_{max}) by 14.29 %, 26.80 %, and 4.60 %, respectively, using the modified Gompertz model. In addition, adding 1, 2, or 3 mg/L of Co NPs reduced the lag phase (λ) by 1.24, 0.59, and 0.89 days, respectively, as compared to the control (1.58 days).

Table 3 Parameters of modified Gompertz model at different concentrations of Co NPs.

Kinetics parameter	Treatments			
	Control	1mg/L Co NPs	2 mg/L Co NPs	3 mg/L Co NPs
R^2	0.998	0.998	0.997	0.998
M_{max} (mL/g VS)	663.9 ±10.37	664.86 ±7.29	695.86 ±8.27	647.92 ±8.26
R_{max} (mL/g VS/d)	27.35 ±0.51	31.26 ±0.56	34.68 ±0.81	28.61 ±0.54
λ (d)	1.58 ±0.19	1.24 ±0.17	0.59 ±0.21	0.89 ±0.18
Predicted biogas yield (mL/g VS)	593.13 ±13.74	620.67 ±19.15	661.50 ±18.08	596.58 ±19.39
Measured biogas yield (mL/g VS)	589.2 ±13.65	629.50 ±19.43	676.50 ±18.50	602.30 ±19.58
Difference between measured and predicted biogas yield (%)	0.66	1.42	2.26	0.95
AIC	135.88	134.00	151.31	134.80

M_{max}: Maximum biogas potential yield; R_{max}: Maximum biogas yield rate; λ: Lag phase; R^2: Correlation Coefficient; AIC: Akaike's information criterion.

Table 4 Parameters of logistic function model at different concentrations of Co NPs.

Kinetics parameter	Treatments			
	Control	1 mg/L Co NPs	2 mg/L Co NPs	3 mg/L Co NPs
R^2	0.996	0.996	0.991	0.995
M_{max} (mL/g VS)	603.56 ±8.62	620.12 ±7.01	660.19 ±9.88	600.42 ±8.02
R_{max} (mL/g VS/d)	28.69 ±0.74	32.23 ±0.85	34.58 ±1.35	29.47 ±0.84
λ (d)	2.43 ±0.28	1.90 ±0.26	0.95 ±0.39	1.55 ±0.30
Predicted biogas yield (mL/g VS)	580.8 ±13.45	607.12 ±18.73	649.29 ±17.75	584.22 ±18.99
Measured biogas yield (mL/g VS)	589.2 ±13.65	629.50 ±19.43	676.50 ±18.5	602.30 ±19.58
Difference between measured and predicted biogas yield (%)	1.43	3.68	4.19	3.09
AIC	157.08	158.41	183.81	161.15

M_{max}: Maximum biogas potential yield; R_{max}: Maximum biogas yield rate; λ: Lag phase; R^2: Correlation Coefficient; AIC: Akaike's information criterion.

The maximum biogas production rate (R_{max}) for the control, 1, 2, and 3 mg/L Co NPs was 28.69, 32.23 (12.33 % increase), 34.58 (20.52 % increase), and 29.47 (2.71 % increase) mL/g VS/d, respectively, for the logistic function model. In addition, the presence of 1, 2, and 3 mg/L Co NPs reduced the lag phase (λ) to 1.90, 0.95, and 1.55 days, respectively, as compared to the control group (2.43 days). Both kinetic models show that Ni NPs increased the rate of biogas production and decreased the lag phase. Tables 3 and 4 show the results of the Akaike Information Criterion (AIC) test for the modified Gompertz and logistic models. The Akaike Information Criterion (AIC) value of the modified Gompertz model is lower, indicating that it is a superior model to utilize in this circumstance.

To derive the hydrolysis rate constant (K) and R^2 in Eq. (4), the hydrolysis of organic materials was assessed using the First-order Kinetic model (Table 5). In general, the model suited the experimental results well, with a coefficient of determination of (0.991–0.993). The presence of 1, 2, and 3 mg/L Co NPs increased the cow dung hydrolysis rate by 72.22 %, 144 %, and 66.66 %, respectively, as compared to

the *K* value of the control treatment. The modified Gompertz model (R^2 = 0.997–0.998) and the logistic function model (R^2 = 0.991–0.996) match the biogas production data well.

Table 5 Parameters of first-order kinetic model at different concentrations of Co NPs.

Kinetics parameter	Treatments			
	Control	1mg/L Co NPs	2 mg/L Co NPs	3 mg/L Co NPs
R^2	0.991	0.989	0.993	0.993
k (d^{-1})	0.018 ±0.003	0.031 ±0.003	0.044 ±0.003	0.030 ±0.003

R^2: Correlation Coefficient; *k*: hydrolysis rate constant.

Conclusions

The performance of AD of cow dung was significantly enhanced by adding Co NPs. The addition of 2 mg/L Co NPs resulted in the highest biogas production (14.81%). Modified Gompertz model had a better fit with the particle biogas production than Logistic Function model. The addition of Co NPs (1–3 mg/L) enhanced the hydrolysis rate (*K*) value by (66.66%-144%) as compared with control. The fertilizer efficiency of effluent with Co NPs was comparable to that of commercial NPK compound fertilizer. Combining kinetic models and experimental measurements can be an optimal strategy for evaluating the impacts of Co NPs additives on AD. In the future, this study can be open a new avenue for the use of effluent containing NPs as fertilizer.

Declarations

Ethical approval

Not applicable

Consent to participate

Not applicable

Consent to publish

Not applicable

Authors contributions

Taha Abdelfattah Mohammed Abdelwahab: Draft preparation, conduct Experiments, Experiment design, Editing. Mahendra Kumar Mohanty: Writing – review & editing, Reviewing. Pradeepta Kumar Sahoo: Data curation. Debaraj Behera: Supervision.

Funding

Not applicable

Competing interests

The authors declare that they have no known competing financial interests or personal relationships that could have appeared to influence the work reported in this paper.

Availability of data and materials

The datasets generated during and/or analysed during the current study are available from the corresponding author on reasonable request.

Acknowledgments

The authors gratefully acknowledge the financial support of Indian Council of Agricultural Research (ICAR). We would also like to acknowledge Odisha University of Agriculture & Technology (OUAT). A special thank you to the College of Agricultural Engineering and Technology Biofuel Energy laboratory.

References

1. Abdelsalam E, Samer M, Attia YA, Abdel-Hadi MA, Hassan HE and Badr Y (2016) Comparison of nanoparticles effects on biogas and methane production from anaerobic digestion of cattle dung slurry. Renew. Energy 87: 592-598. DOI: 10.1016/j.renene.2015.10.053.
2. Abdelsalam E, Samer M, Attia YA, Abdel-Hadi MA, Hassan HE and Badr Y (2017a) Effects of Co and Ni nanoparticles on biogas and methane production from anaerobic digestion of slurry. Energy Convers. Manag. 141:108-119. DOI: 10.1016/j.enconman.2016.05.051.
3. Abdelsalam E, Samer M, Attia YA, Abdel-Hadi MA, Hassan HE and Badr Y (2017b) Influence of zero valent iron nanoparticles and magnetic iron oxide nanoparticles on biogas and methane production from anaerobic digestion of manure. Energy 120: 842-853. DOI: 10.1016/j.energy.2016.11.137.
4. Abdelwahab T A M, Mohanty M K, Sahoo P K and Behera D (2021a) Metal nanoparticle mixtures to improve the biogas yield of cattle manure. Biomass Convers Bior. 1-12. DOI: 10.1007/s13399-021-01286-3.
5. Abdelwahab T A M, Mohanty M K, Sahoo P K and Behera D (2021b) Impact of nickel nanoparticles on biogas production from cattle manure. Biomass Convers Bior. 1-14. DOI: 10.1007/s13399-021-01460-7.

6. Abdelwahab TA M, Mohanty M K, Sahoo P K and Behera D (2020b) Impact of iron nanoparticles on biogas production and effluent chemical composition from anaerobic digestion of cattle manure. Biomass Convers Bior. 1-13. DOI: 10.1007/s13399-020-00985-7.
7. Abdelwahab, T. A. M., Mohanty, M. K., Sahoo, P. K., & Behera, D (2020a) Application of nanoparticles for biogas production: Current status and perspectives. Energ. Source. Part. A. 1-13. DOI: 10.1080/15567036.2020.1767730.
8. Abdulla HA, Minor EC, Dias RF and Hatcher PG (2010) Changes in the compound classes of dissolved organic matter along an estuarine transect: a study using FTIR and 13C NMR. Geochimica et Cosmochimica Acta 74(13): 3815-3838. DOI: 10.1016/j.gca.2010.04.006.
9. Ahn HK, Smith MC, Kondrad SL and White JW (2010) Evaluation of biogas production potential by dry anaerobic digestion of switchgrass–animal manure mixtures. Biotechnol. Appl. Biochem. 160(4): 965-975. DOI: 10.1007/s12010-009-8624-x.
10. Ajay CM, Mohan S, Dinesha P and Rosen MA (2020) Review of impact of nanoparticle additives on anaerobic digestion and methane generation. Fuel 277:118234. DOI: 10.1016/j.fuel.2020.118234.
11. Ali A, Mahar RB, Abdelsalam EM, Sherazi STH (2019) Kinetic modeling for bioaugmented anaerobic digestion of the organic fraction of municipal solid waste by using Fe_3O_4 nanoparticles. Waste Biomass Valori. 10(11): 3213-3224. DOI: 10.1007/s12649-018-0375-x.
12. Amen TW, Eljamal O, Khalil AM, Sugihara Y and Matsunaga N (2018) Methane yield enhancement by the addition of new novel of iron and copper-iron bimetallic nanoparticles. Chem. Eng. Process. 130: 253-261. DOI: 10.1016/j.cep.2018.06.020
13. APHA (1995) Standard Methods for Examination of Water and Wastewater, American Public Health Association APHA, Washington, DC, USA.
14. APHA (2005) Standard Methods for Examination of Water and Wastewater. 21st ed. APHA, Washington, DC, USA.
15. Bayr S, Pakarinen O, Korppoo A, Liuksia S, Väisänen A, Kaparaju P and Rintala J (2012) Effect of additives on process stability of mesophilic anaerobic monodigestion of pig slaughterhouse waste. Bioresour. Technol. 120: 106-113. DOI: 10.1016/j.biortech.2012.06.009.
16. Bedoić R, Špehar A, Puljko, J, Čuček L, Ćosić B, Pukšec T and Duić N (2020) Opportunities and challenges: Experimental and kinetic analysis of anaerobic co-digestion of food waste and rendering industry streams for biogas production. Renew. Sustain. Energy Rev. 130:109951. DOI: 10.1016/j.rser.2020.109951.
17. Boer JL, Mulrooney SB and Hausinger RP (2014) Nickel-dependent metalloenzymes, Archives of biochemistry and biophysics 544:142-152. DOI: 10.1016/j.abb.2013.09.002.
18. Chen Y, Cheng JJ and Creamer KS (2008) Inhibition of anaerobic digestion process: a review. Bioresour. Technol. 99(10): 4044-4064. DOI: 10.1016/j.biortech.2007.01.057.
19. Chowdhury T, Chowdhury H, Hossain N, Ahmed A, Hossen MS, Chowdhury P, Thirugnanasambandam M and Saidur R (2020) Latest advancements on livestock waste management and biogas production: Bangladesh's perspective. J. Clean. Prod. 122818. DOI: 10.1016/j.jclepro.2020.122818.

20. Deepanraj B, Sivasubramanian V and Jayaraj S (2017) Effect of substrate pretreatment on biogas production through anaerobic digestion of food waste. Int. J. Hydrog. Energy. 42(42): 26522-26528. DOI: 10.1016/j.ijhydene.2017.06.178.
21. Demirel B and Scherer P (2011) Trace element requirements of agricultural biogas digesters during biological conversion of renewable biomass to methane. Biomass Bioenergy 35(3): 992-998. DOI: 10.1016/j.biombioe.2010.12.022.
22. Donoso-Bravo, A., P´erez-Elvira, S.I., Fdz-Polanco, F (2010) Application of simplified models for anaerobic biodegradability tests. Evaluation of pre-treatment processes. Chem. Eng. J. 160(2): 607-614. DOI: 10.1016/j.cej.2010.03.082.
23. Facchin V, Cavinato C, Fatone F, Pavan P, Cecchi F, Bolzonella D (2013) Effect of trace element supplementation on the mesophilic anaerobic digestion of foodwaste in batch trials: The influence of inoculum origin. Biochem. Eng. J. 70: 71–77. DOI: 10.1016/j.bej.2012.10.004.
24. Gamage IH, Jonker A, Zhang X and Yu P (2014) Non-destructive analysis of the conformational differences among feedstock sources and their corresponding co-products from bioethanol production with molecular spectroscopy. Spectrochim. Acta A Mol. Biomol. Spectrosc. 118: 407-421. DOI: 10.1016/j.saa.2013.08.095.
25. Ghosh P, Kumar M, Kapoor R, Kumar SS, Singh L, Vijay V, Vijay VK, Kumar V and Thakur IS (2020) Enhanced biogas production from municipal solid waste via co-digestion with sewage sludge and metabolic pathway analysis. Bioresour. Technol. 296: 122275. DOI: 10.1016/j.biortech.2019.122275.
26. Hassanein A, Lansing S and Tikekar R (2019) Impact of metal nanoparticles on biogas production from poultry litter. Bioresour. Technol. 275: 200-206. DOI: 10.1016/j.biortech.2018.12.048.
27. Kiran EU, Trzcinski AP and Liu Y (2015) Enhancing the hydrolysis and methane production potential of mixed food waste by an effective enzymatic pretreatment. Bioresour. Technol. 183: 47-52. DOI: 10.1016/j.biortech.2015.02.033.
28. Kothari R, Pandey AK, Kumar S, Tyagi VV and Tyagi SK (2014) Different aspects of dry anaerobic digestion for bio-energy: An overview. Renew. Sustain. Energy Rev. 39: 174-195. DOI: 10.1016/j.rser.2014.07.011.
29. Liu A, Xu S, Lu C, Peng P, Zhang Y, Feng D and Liu Y (2014) Anaerobic fermentation by aquatic product wastes and other auxiliary materials. Clean Technol Environ Policy 16(2): 415-421. DOI: 10.1007/s10098-013-0640-4.
30. Madsen M, Holm-Nielsen JB and Esbensen KH (2011) Monitoring of anaerobic digestion processes: A review perspective. Renew. Sustain. Energy Rev. 15(6): 3141-3155. DOI: 10.1016/j.rser.2011.04.026.
31. Mishra, R.K., Mohanty, K. (2018) Pyrolysis kinetics and thermal behavior of waste sawdust biomass using thermogravimetric analysis. Bioresour. Technol. 251: 63–74. DOI: 10.1016/j.biortech.2017.12.029.
32. Möller K and Müller T (2012) Effects of anaerobic digestion on digestate nutrient availability and crop growth: a review. Eng. Life Sci. 12(3): 242-257. DOI:10.1002/elsc.201100085.

33. Muyzer G and Stams AJ (2008) The ecology and biotechnology of sulphate-reducing bacteria. Nat Rev Microbiol 6(6): 441-454. DOI: 10.1038/nrmicro1892.
34. Nguyen D, Visvanathan C, Jacob P and Jegatheesan V (2015) Effects of nano cerium (IV) oxide and zinc oxide particles on biogas production. Int. Biodeterior. Biodegradation 102 :165-171. DOI: 10.1016/j.ibiod.2015.02.014.
35. O'Keeffe S and Thrän D (2020) Energy Crops in Regional Biogas Systems: An Integrative Spatial LCA to Assess the Influence of Crop Mix and Location on Cultivation GHG Emissions. Sustainability 12(1): 237. DOI: 10.3390/SU12010237.
36. Qiang H, Lang DL and Li YY (2012) High-solid mesophilic methane fermentation of food waste with an emphasis on Iron, Cobalt, and Nickel requirements. Bioresour. Technol. 103(1): 21-27. DOI: 10.1016/j.biortech.2011.09.036.
37. Rawlings JO, Pantula SG and Dickey DA (2001) Applied regression analysis: a research tool, Springer Science & Business Media.
38. Romero-Güiza MS, Vila J, Mata-Alvarez J, Chimenos JM and Astals S (2016) The role of additives on anaerobic digestion: a review. Renew. Sustain. Energy Rev. 58: 1486-1499. DOI: 10.1016/j.rser.2015.12.094.
39. Romsaiyud A, Songkasiri W, Nopharatana A and Chaiprasert P (2009) Combination effect of pH and acetate on enzymatic cellulose hydrolysis. J Environ Sci.21(7): 965-970. DOI: 10.1016/S1001-0742(08)62369-4.
40. Roussel J (2013) Metal behaviour in anaerobic sludge digesters supplemented with trace nutrients (Doctoral dissertation, University of Birmingham).
41. Sevcu A, El-Temsah YS, Joner EJ and Cernik M (2011) Oxidative stress induced in microorganisms by zero-valent iron nanoparticles. Microbes Environ. 26(4): 271-281. DOI: 10.1264/jsme2.me11126.
42. Suanon F, Sun Q, Li M, Cai X, Zhang Y, Yan Y and Yu CP (2017) Application of nanoscale zero valent iron and iron powder during sludge anaerobic digestion: Impact on methane yield and pharmaceutical and personal care products degradation. J. Hazard. Mater. 321: 47-53. DOI: 10.1016/j.jhazmat.2016.08.076.
43. Syaichurrozi I and Sumardiono S (2013) Predicting kinetic model of biogas production and biodegradability organic materials: biogas production from vinasse at variation of COD/N ratio. Bioresour. Technol. 149: 390-397. DOI: 10.1016/j.biortech.2013.09.088.
44. Tamburini E, Gaglio M, Castaldelli G and Fano EA (2020) Biogas from Agri-Food and Agricultural Waste Can Appreciate Agro-Ecosystem Services: The Case Study of Emilia Romagna Region. Sustainability 12(20): 8392. DOI: 10.3390/su12208392.
45. Thauer RK, Kaster AK, Seedorf H, Buckel W and Hedderich R (2008) Methanogenic archaea: ecologically relevant differences in energy conservation. *Nat. Rev. Microbiol.* 6(8): 579-591. DOI:10.1038/nrmicro1931.
46. Trifunović D, Schuchmann K and Müller V (2016) Ethylene glycol metabolism in the acetogen Acetobacterium woodii. J. Bacteriol. 198(7): 1058-1065. DOI: 10.1128/JB.00942-15.

47. Wang QL, Li W, Gao X and Li SJ (2016) Life cycle assessment on biogas production from straw and its sensitivity analysis. Bioresour. Technol. 201: 208-214. DOI: 1-10. 10.1038/srep25857.
48. Wei L, Qin K, Ding J, Xue M, Yang C, Jiang J and Zhao Q (2019) Optimization of the co-digestion of sewage sludge, maize straw and cow manure: microbial responses and effect of fractional organic characteristics. Sci. Rep. 9(1): 1-10. DOI: 10.1016/j.chemosphere.2014.08.060.
49. Wong CS and Li WK (1998) A note on the corrected Akaike information criterion for threshold autoregressive models. J. Time Ser. Anal. 19(1): 113-124. DOI: 10.1111/1467-9892.00080.
50. Zaidi AA, RuiZhe F, Shi Y, Khan SZ and Mushtaq K (2018) Nanoparticles augmentation on biogas yield from microalgal biomass anaerobic digestion. Int. J. Hydrog. Energy. 43(31): 14202-14213. DOI: 10.1016/j.ijhydene.2018.05.132.
51. Zandvoort MH, Van Hullebusch ED, Fermoso FG and Lens PNL (2006) Trace metals in anaerobic granular sludge reactors: bioavailability and dosing strategies. Eng. Life Sci. 6(3): 293-301. DOI: 10.1002/elsc.200620129.
52. Zhang M and Zang L (2019) A review of interspecies electron transfer in anaerobic digestion, In IOP Conference Series: Earth and Environmental Science. 310 (4): 042026, IOP Publishing.
53. Zhang W, Wei Q, Wu S, Qi D, Li W, Zuo Z, Dong R (2014) Batch anaerobic co-digestion of pig manure with dewatered sewage sludge under mesophilic conditions. Appl. Energy 128: 175-183. DOI: 10.1016/j.apenergy.2014.04.071.

Figures

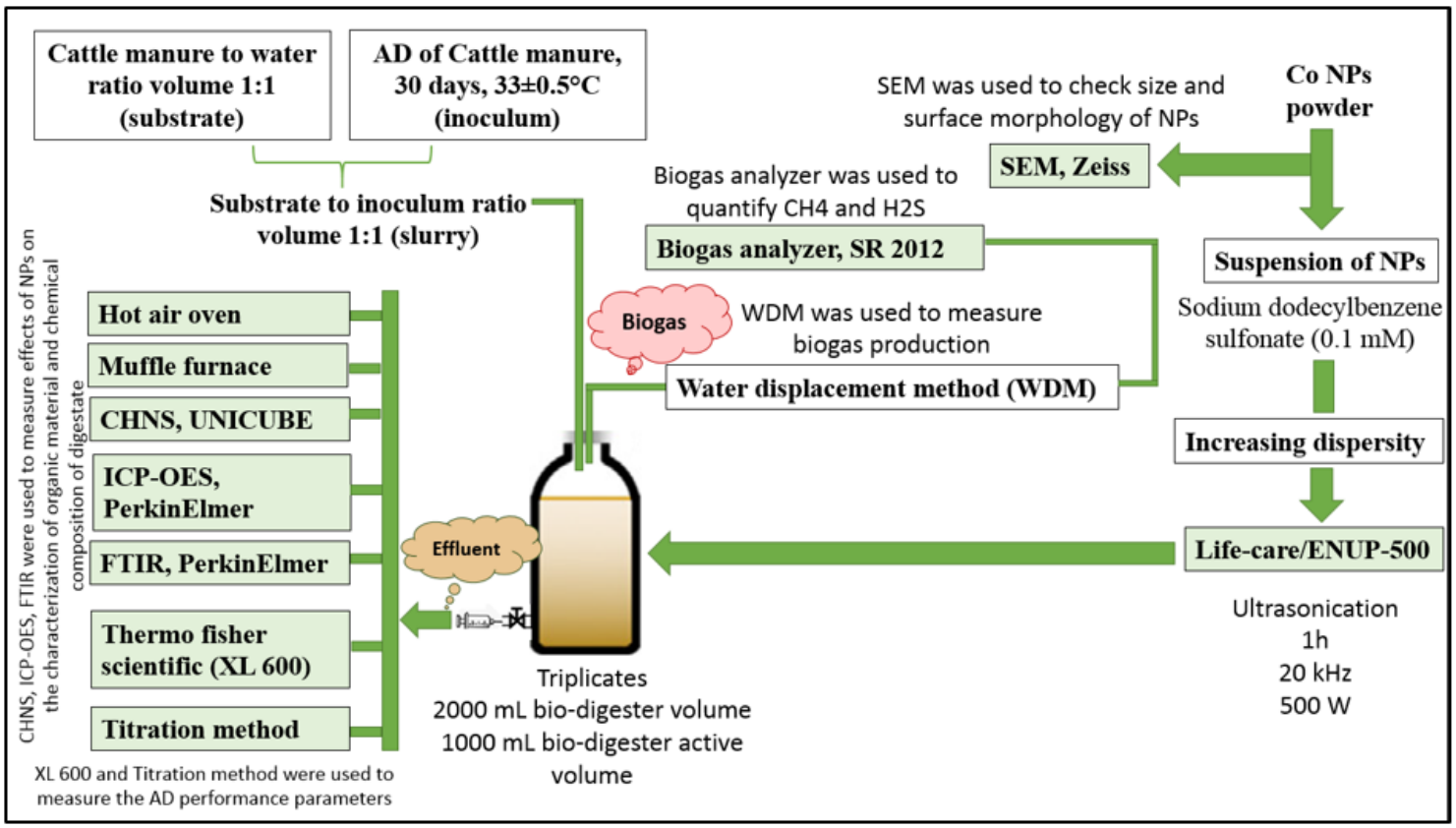

Figure 1

The methods used in experiments.

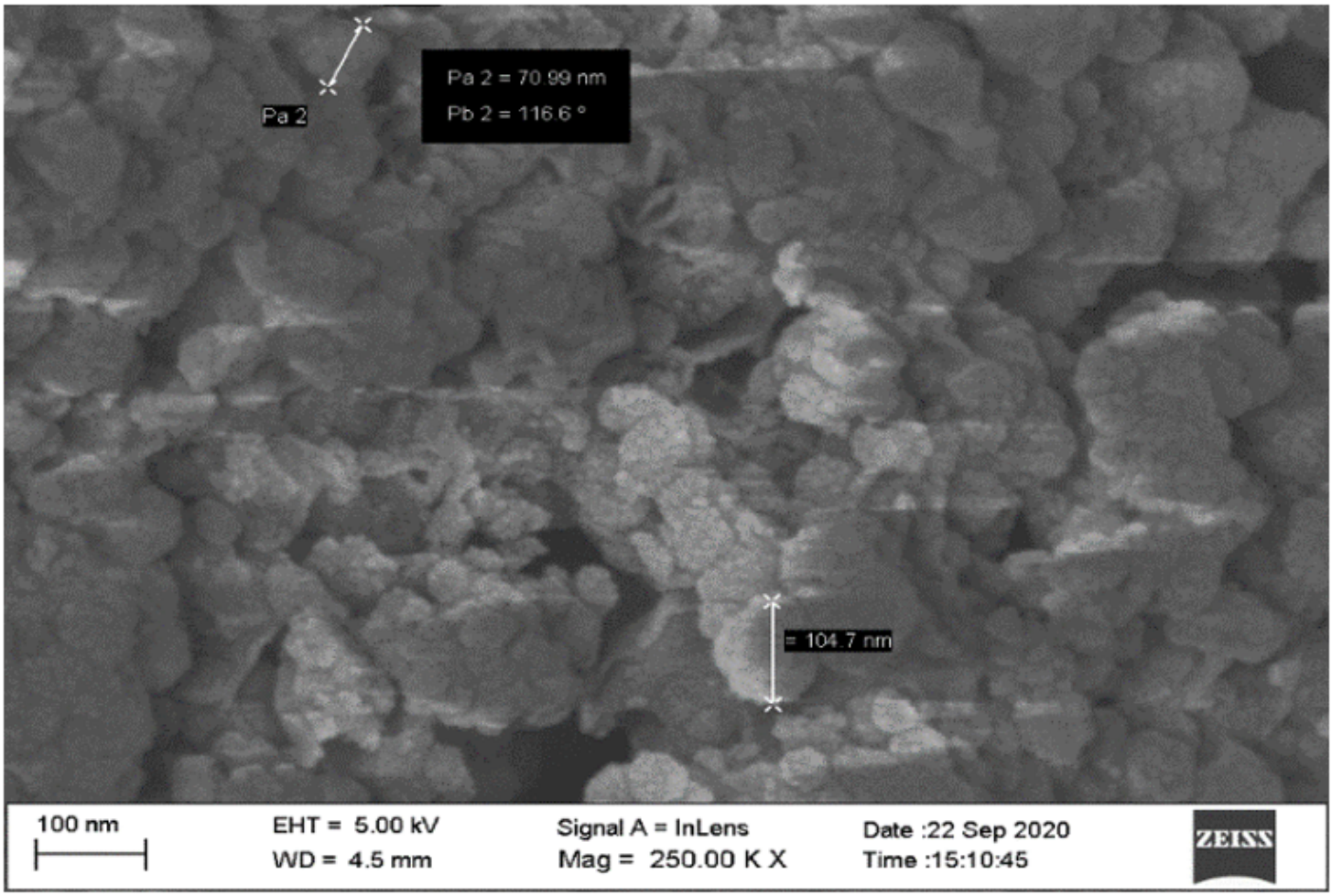

Figure 2

FESEM image of the Co NPs.

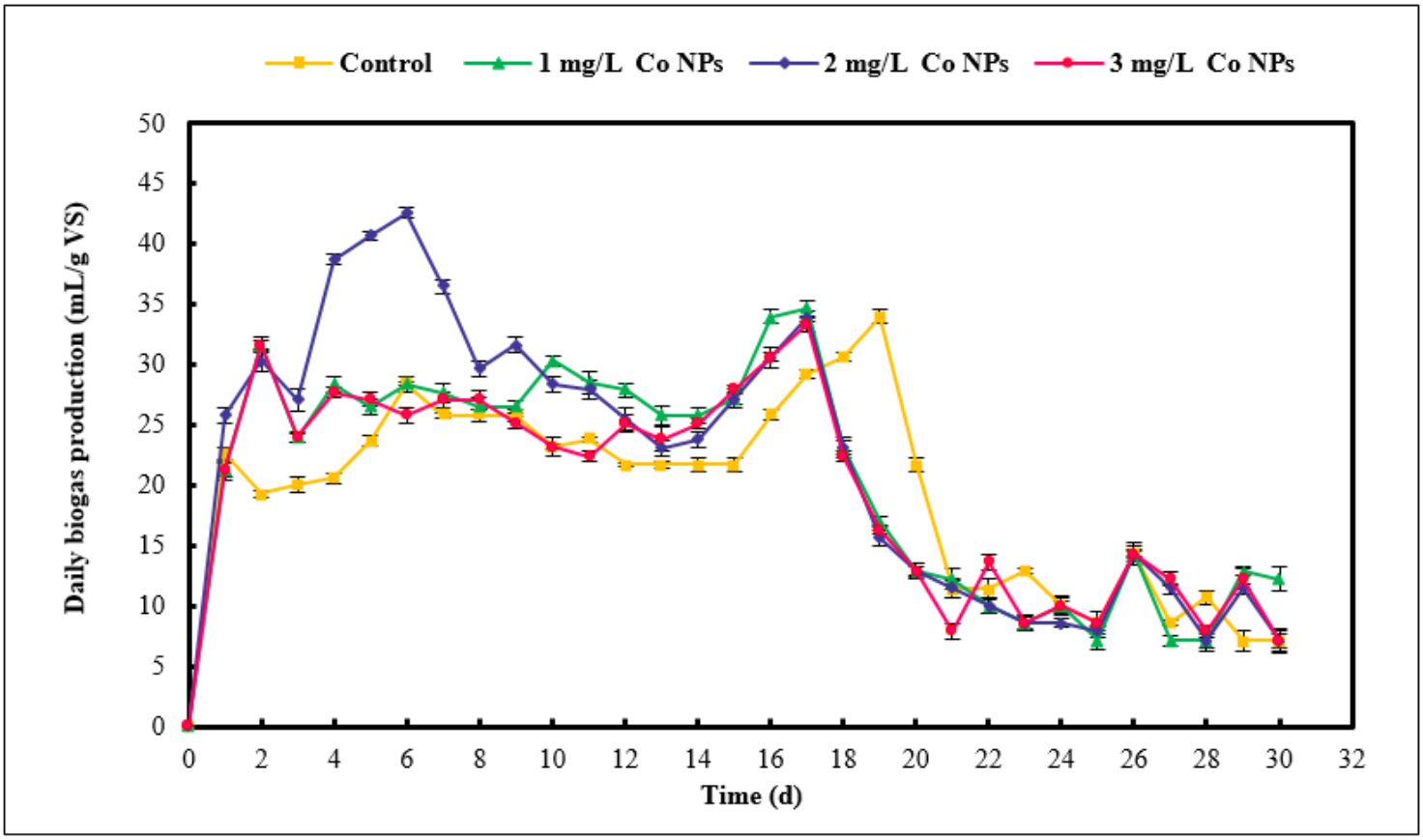

Figure 3

Effect of different Co NPs concentrations on daily biogas production.

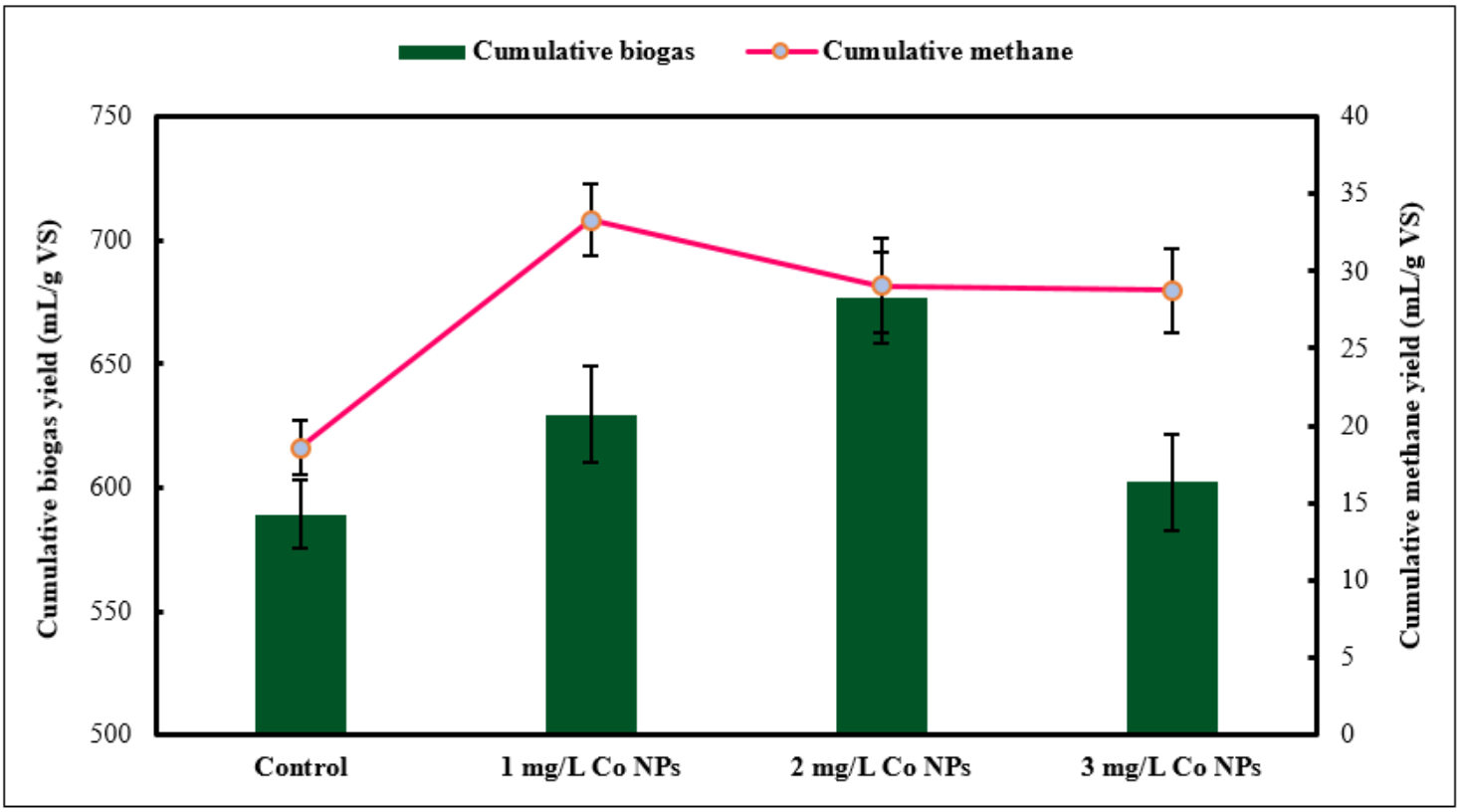

Figure 4

Effect of different Co NPs concentrations on cumulative biogas and methane production.

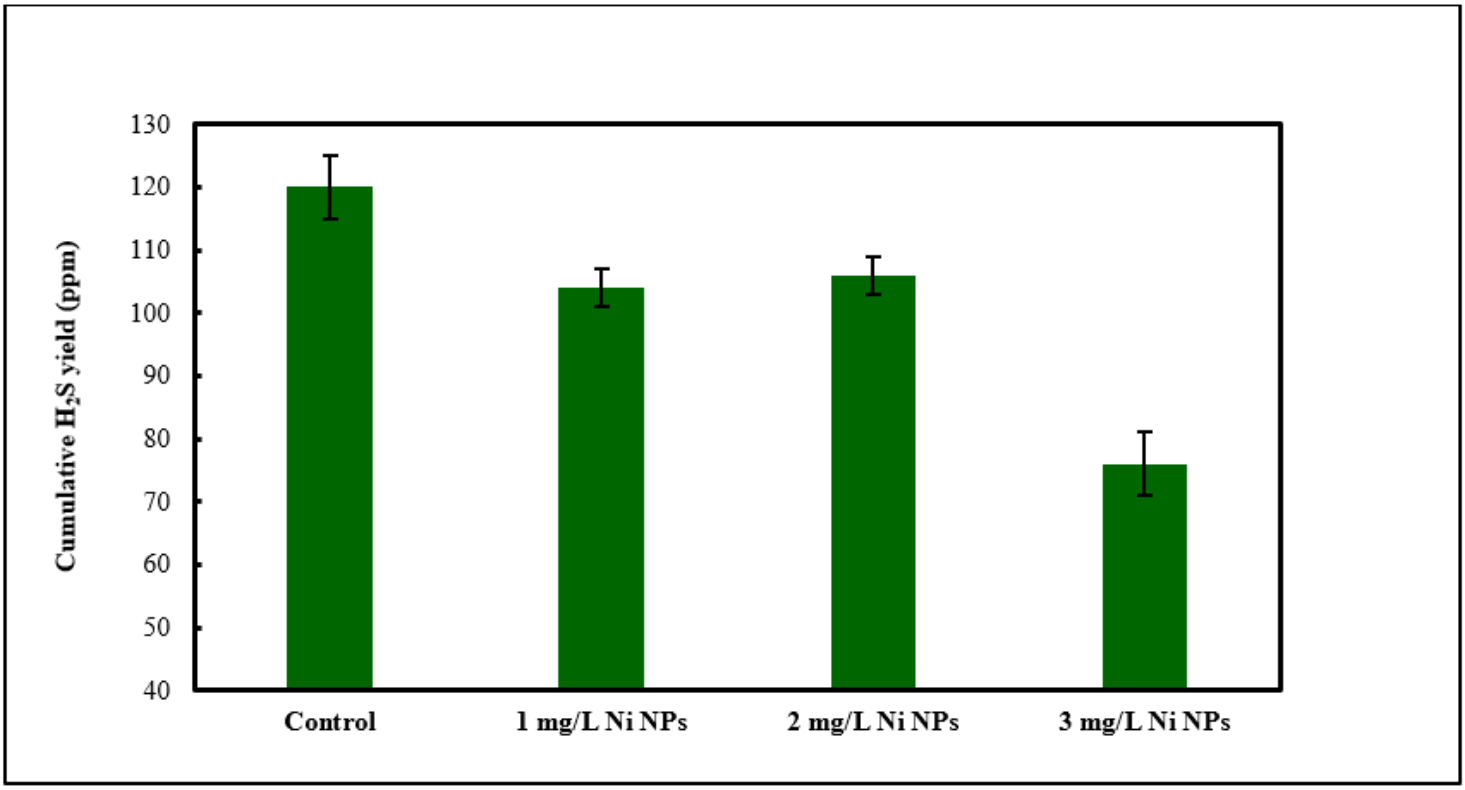

Figure 5

Effect of different Co NPs concentrations on cumulative H2S production.

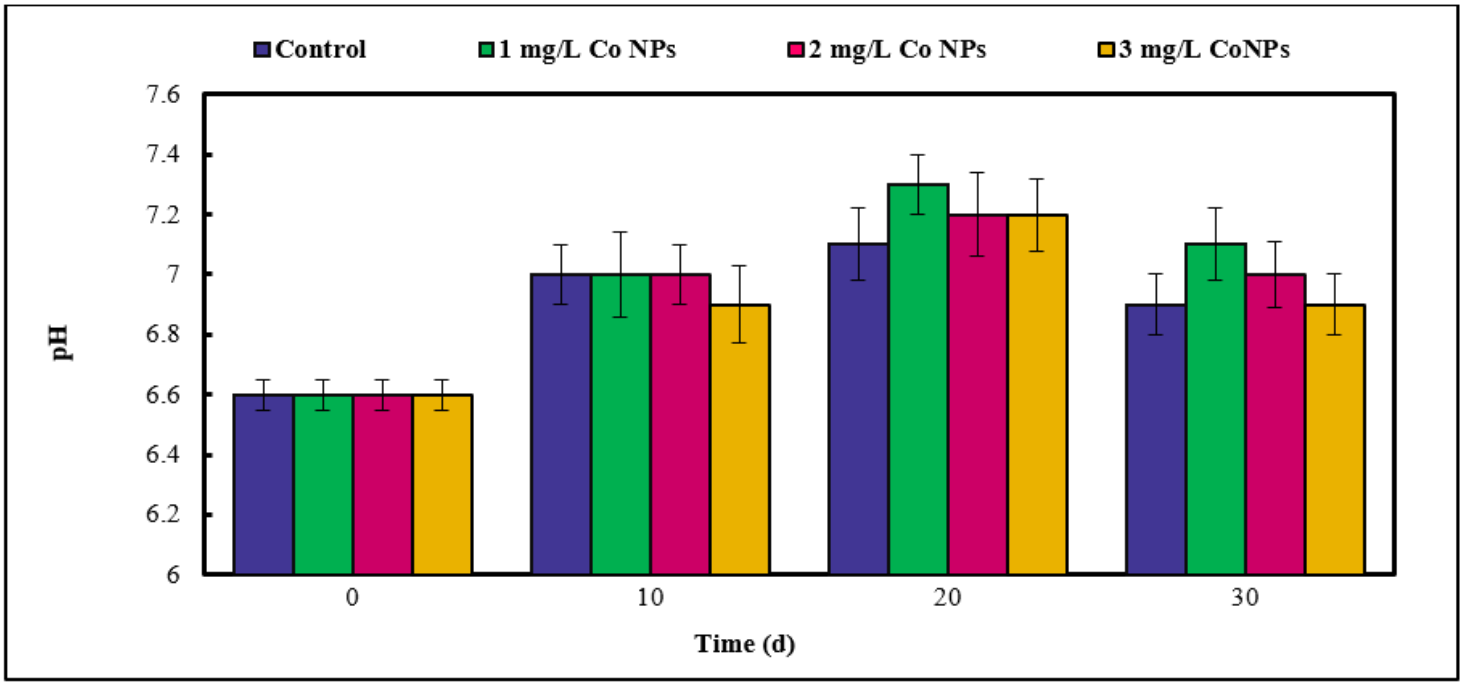

Figure 6

Effect of different Co NPs concentrations on pH.

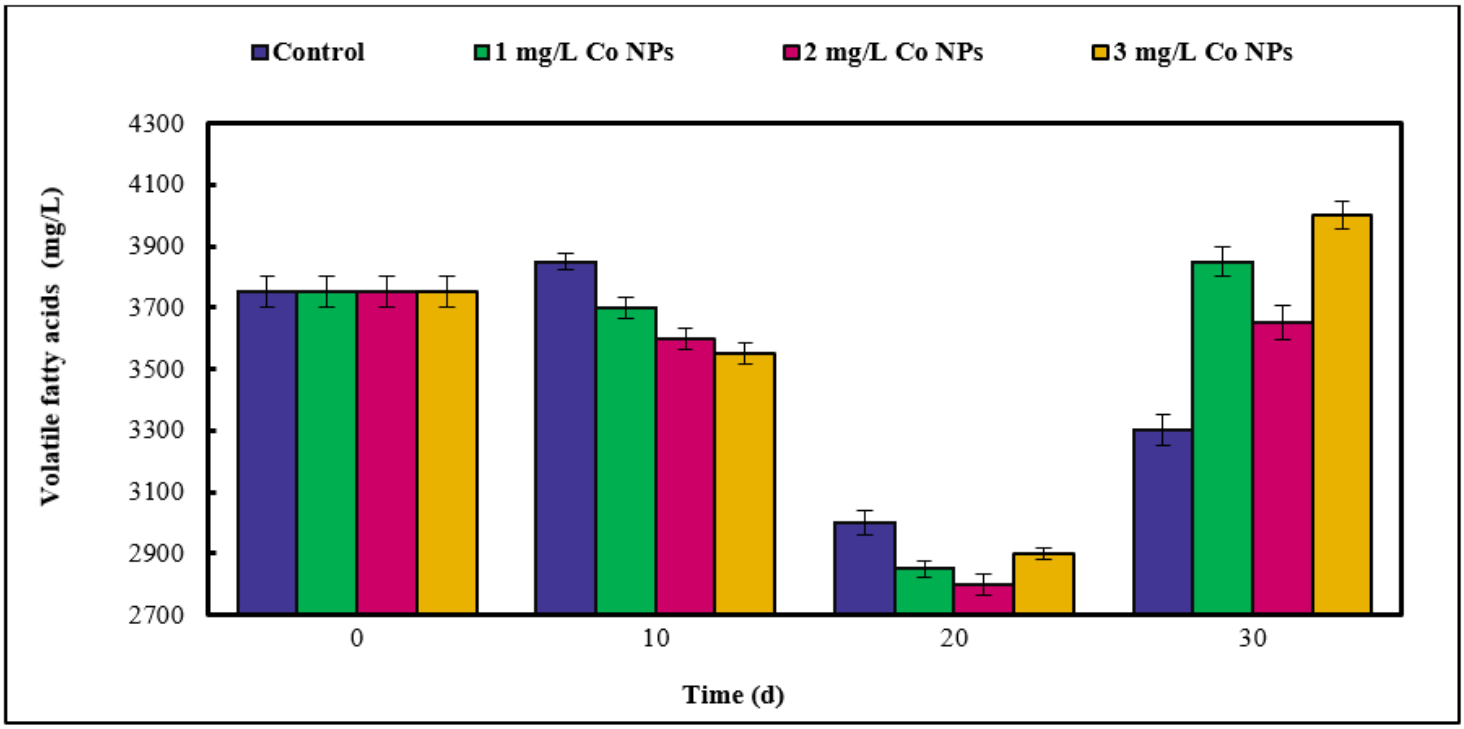

Figure 7

Effect of different Co NPs concentrations on volatile fatty acids.

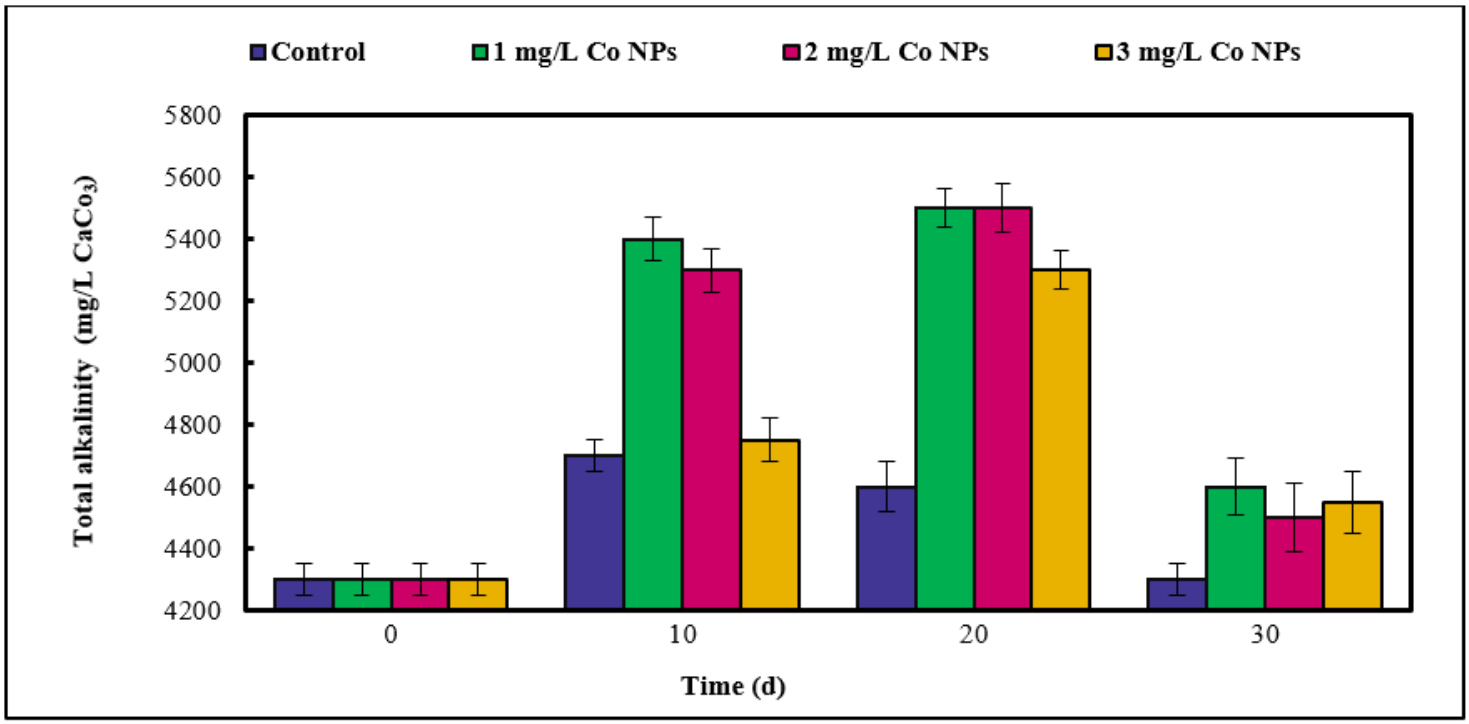

Figure 8

Effect of different Co NPs concentrations on total alkalinity.

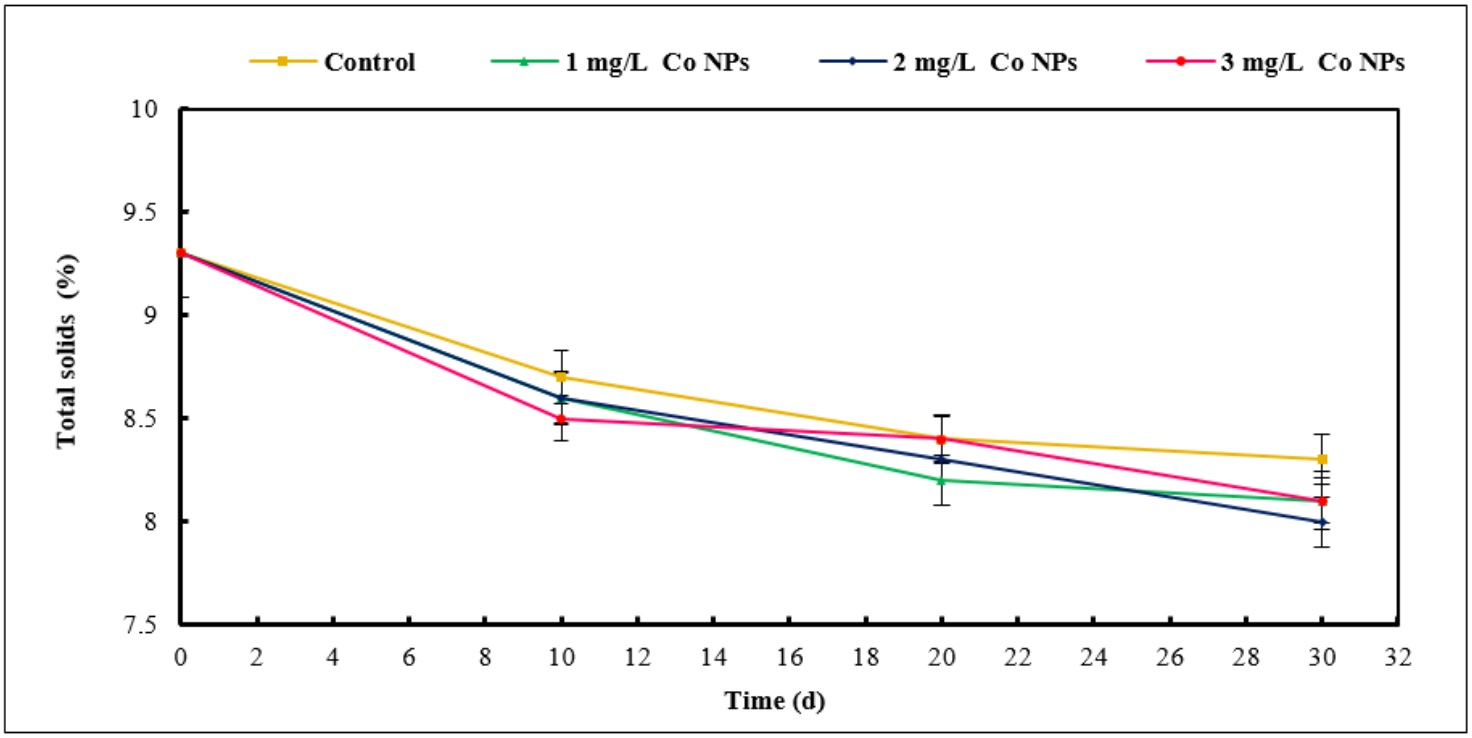

Figure 9

Effect of different Co NPs concentrations on total solids.

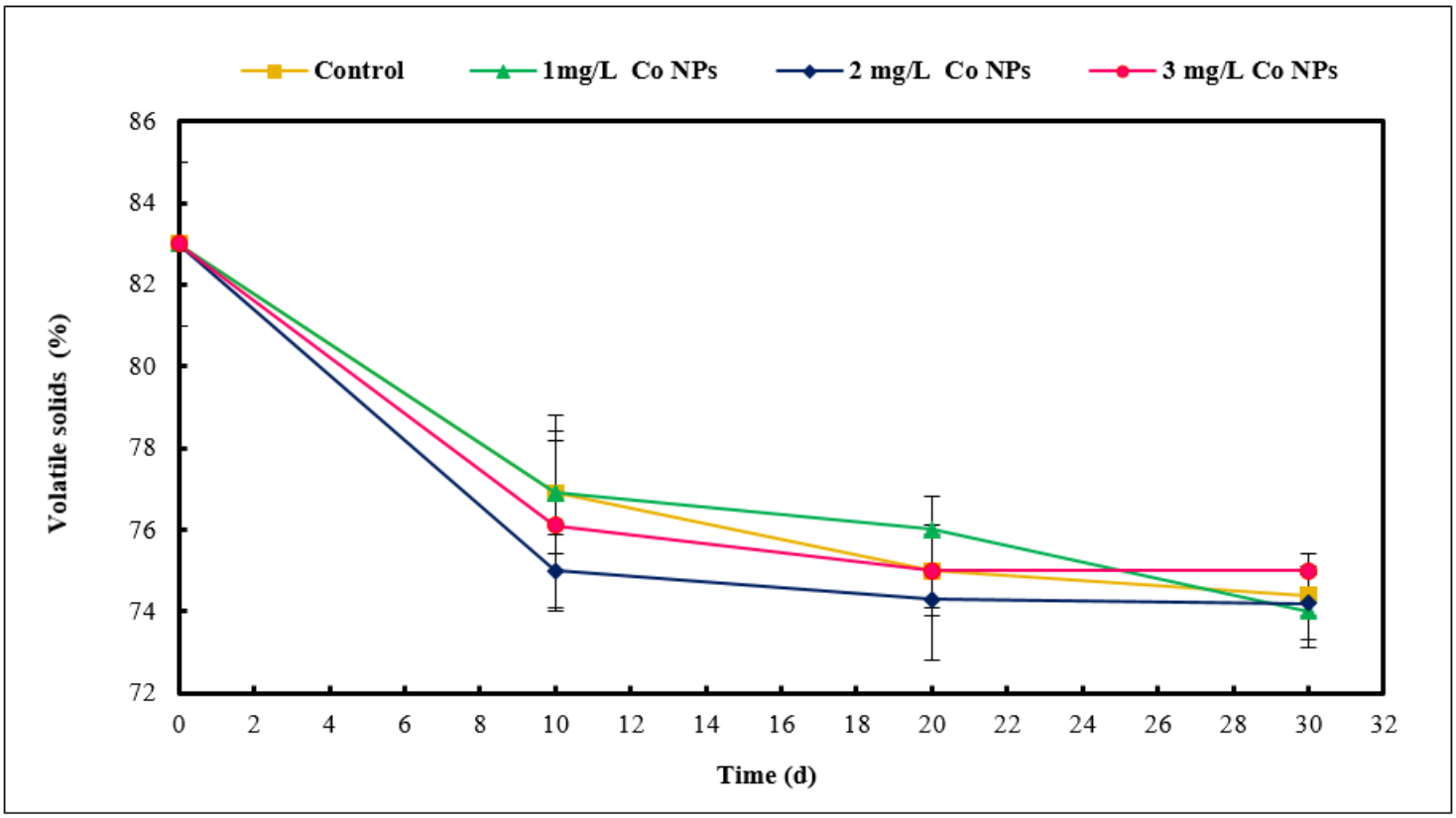

Figure 10

Effect of different Co NPs concentrations on volatile solids.

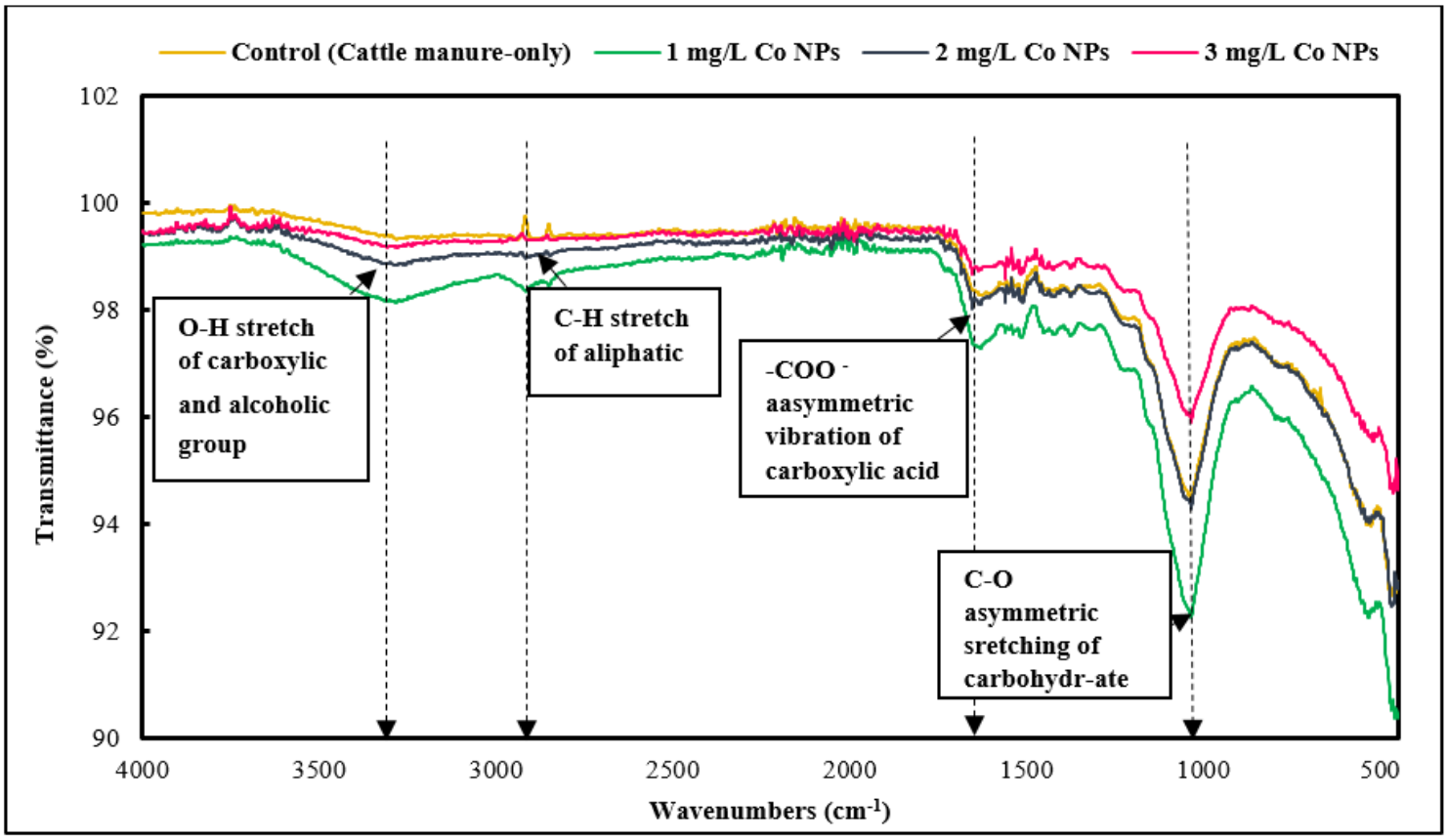

Figure 11

The FTIR spectra of the effluent with different concentrations of Co NPs.

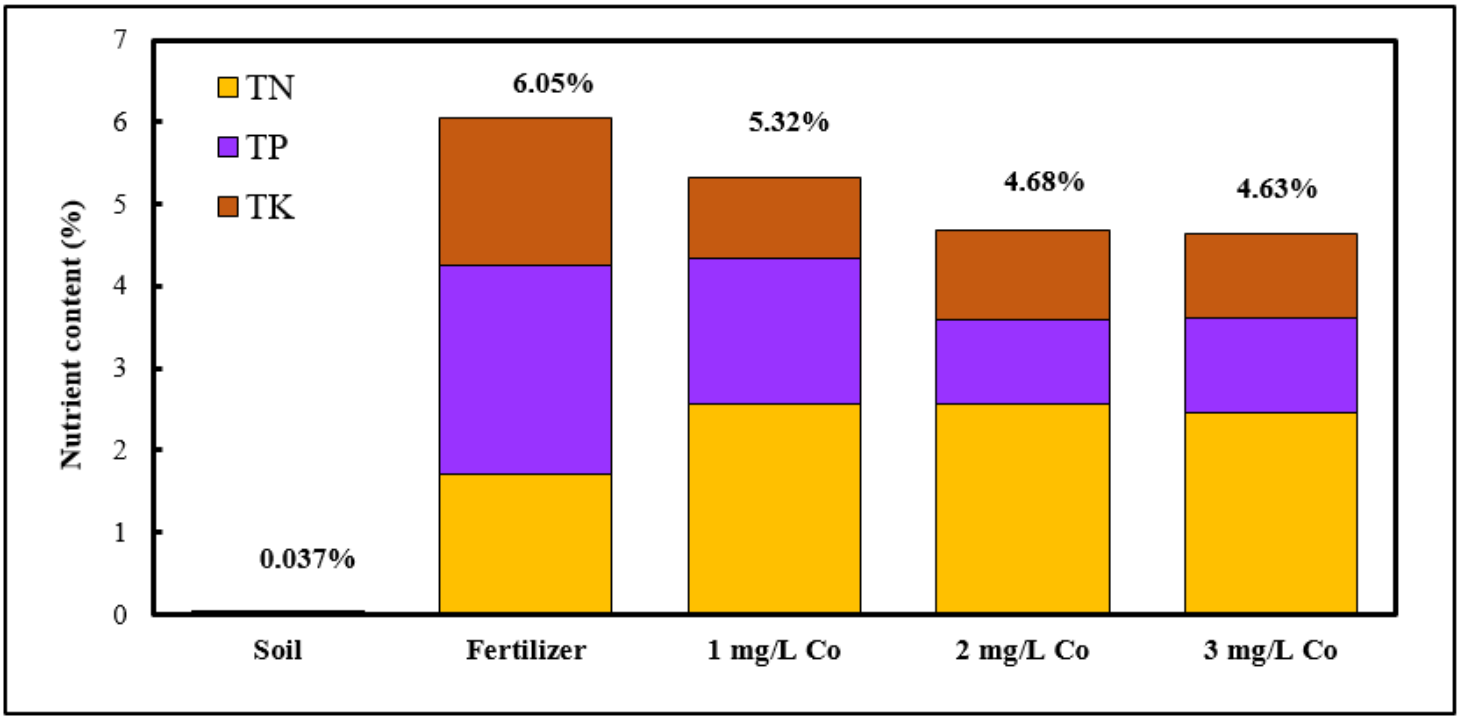

Figure 12

The NPK contents of soil, commercial bio-organic fertilizer and the effluent with different Co NPs concentrations.

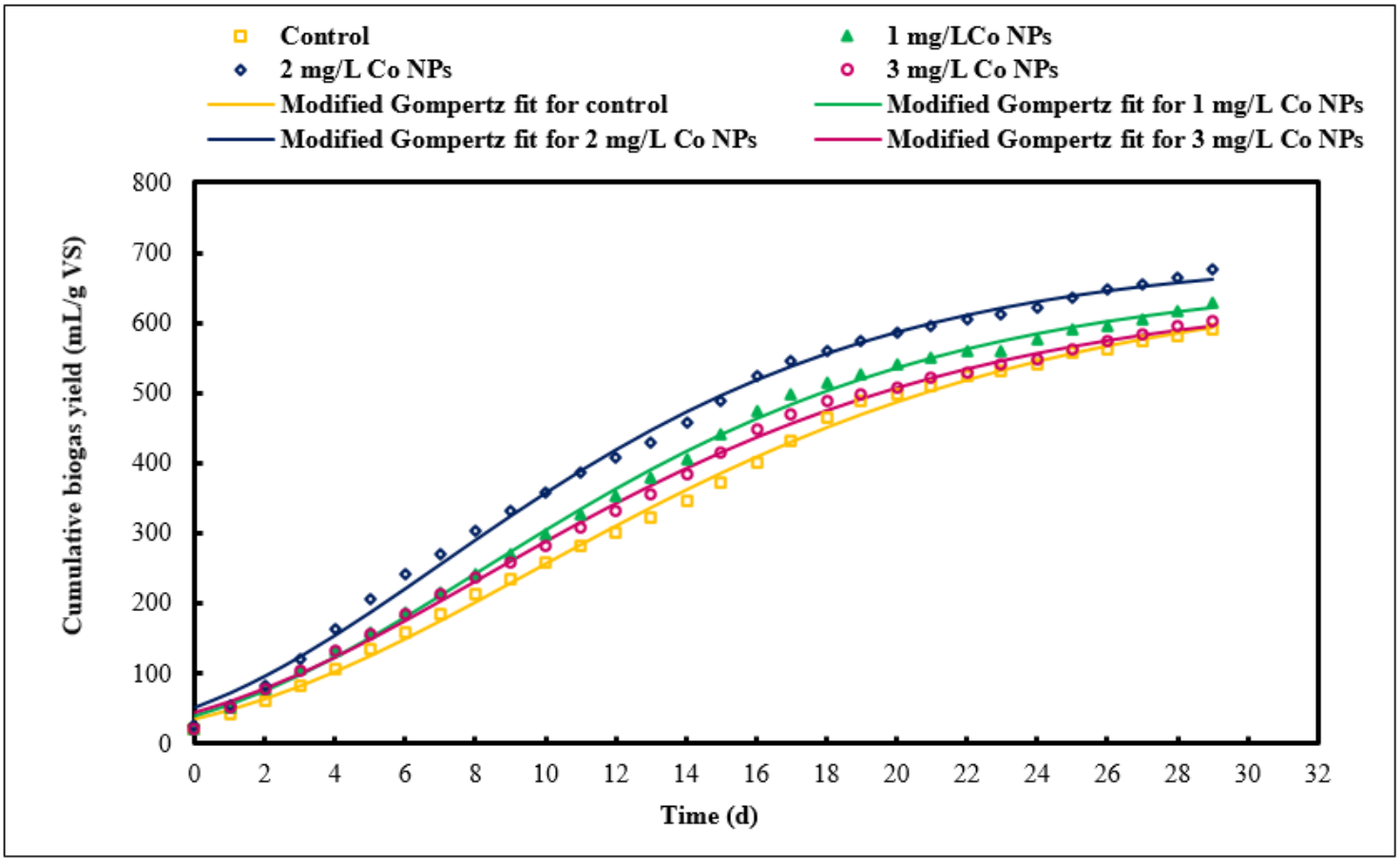

Figure 13

The comparison of experimental and predicted biogas production by using modified Gompertz model with different concentrations of Co NPs.

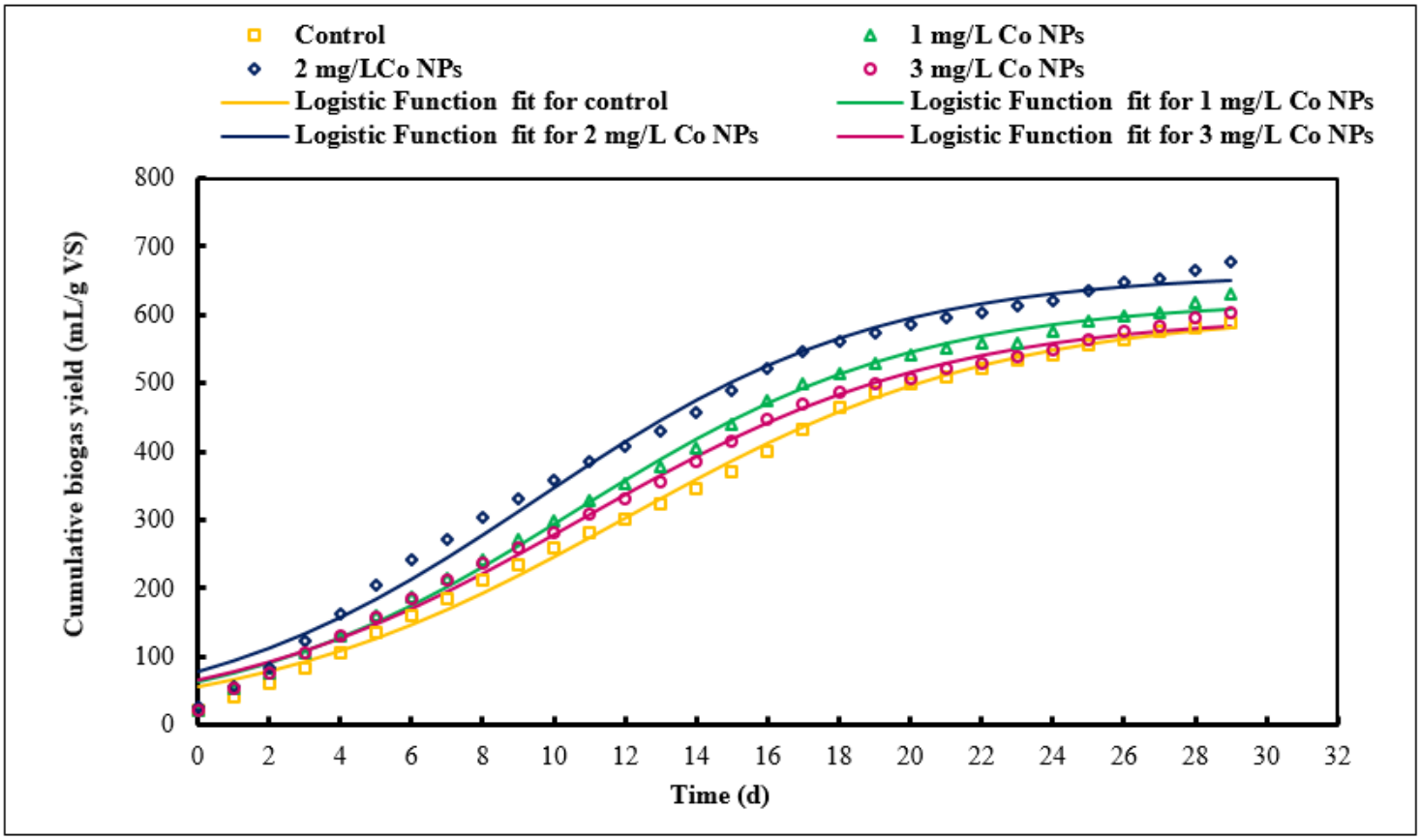

Figure 14

The comparison of experimental and predicted biogas production by using logistic function model with different concentrations of Co NPs.

Supplementary Files

This is a list of supplementary files associated with this preprint. Click to download.

- Graphicalabstract.docx